



Since January 2020 Elsevier has created a COVID-19 resource centre with free information in English and Mandarin on the novel coronavirus COVID-19. The COVID-19 resource centre is hosted on Elsevier Connect, the company's public news and information website.

Elsevier hereby grants permission to make all its COVID-19-related research that is available on the COVID-19 resource centre - including this research content - immediately available in PubMed Central and other publicly funded repositories, such as the WHO COVID database with rights for unrestricted research re-use and analyses in any form or by any means with acknowledgement of the original source. These permissions are granted for free by Elsevier for as long as the COVID-19 resource centre remains active.



## ORIGINAL ARTICLE

# Fluorescence spectrophotometry for COVID-19 determination in clinical swab samples



Kartika A. Madurani<sup>a</sup>, Suprpto<sup>a</sup>, Muhammad Yudha Syahputra<sup>a</sup>, Ika Puspita<sup>b</sup>, Abdul Hadi Furqoni<sup>c</sup>, Listya Puspasari<sup>a</sup>, Hafildatur Rosyidah<sup>a</sup>, Agus Muhamad Hatta<sup>b</sup>, Juniastuti<sup>d,e</sup>, Maria Inge Lusida<sup>d,e</sup>, Masato Tominaga<sup>f</sup>, Fredy Kurniawan<sup>a,\*</sup>

<sup>a</sup> Laboratory of Instrumentation and Analytical Science, Chemistry Department, Faculty of Science and Data Analytics, Institut Teknologi Sepuluh Nopember, Surabaya 60111, Indonesia

<sup>b</sup> Photonics Engineering Laboratory, Department of Engineering Physics, Faculty of Industrial Technology and Systems Engineering, Institut Teknologi Sepuluh Nopember, Surabaya 60111, Indonesia

<sup>c</sup> Human Genetic Laboratory, Institute of Tropical Disease, Airlangga University, Surabaya 60115, Indonesia

<sup>d</sup> Faculty of Medicine, Airlangga University, Surabaya 60131, Indonesia

<sup>e</sup> Institute of Tropical Disease, Airlangga University, Surabaya 60115, Indonesia

<sup>f</sup> Department of Chemistry and Applied Chemistry, Graduate School of Science and Engineering, Saga University, Saga 840-8502, Japan

Received 12 January 2022; accepted 25 May 2022

Available online 30 May 2022

## KEYWORDS

COVID-19;  
SARS-CoV-2;  
Fast analysis;  
Fluorescence spectroscopy;  
Excitation;  
Emission

**Abstract** Considering the limitations of the assays currently available for the detection of severe acute respiratory syndrome coronavirus 2 (SARS-CoV-2) and its emerging variants, a simple and rapid method using fluorescence spectrophotometry was developed to detect coronavirus disease 2019 (COVID-19). Forty clinical swab samples were collected from the nasopharyngeal and oropharyngeal cavities of COVID-19-positive and -negative. Each sample was divided into two parts. The first part of the samples was analyzed using reverse transcription-polymerase chain reaction (RT-qPCR) as the control method to identify COVID-19-positive and -negative samples. The second part of the samples was analyzed using fluorescence spectrophotometry. Fluorescence measurements were performed at excitation and emission wavelengths ranging from 200 to 800 nm. Twenty COVID-19-positive samples and twenty COVID-19-negative samples were detected based on RT-qPCR results. The fluorescence spectrum data indicated that the COVID-19-positive and

\* Corresponding author.

E-mail addresses: [fredy@chem.its.ac.id](mailto:fredy@chem.its.ac.id), [fredykurniawan5@gmail.com](mailto:fredykurniawan5@gmail.com) (F. Kurniawan).

Peer review under responsibility of King Saud University.



-negative samples had significantly different characteristics. All positive samples could be distinguished from negative samples by fluorescence spectrophotometry. Principal component analysis showed that COVID-19-positive samples were clustered separately from COVID-19-negative samples. The specificity and accuracy of this experiment reached 100%. Limit of detection (LOD) obtained 42.20 copies/ml (Ct value of 33.65 cycles) for E gene and 63.60 copies/ml (Ct value of 31.36 cycles) for ORF1ab gene. This identification process only required 4 min. Thus, this technique offers an efficient and accurate method to identify an individual with active SARS-CoV-2 infection and can be easily adapted for the early investigation of COVID-19, in general.

© 2022 The Author(s). Published by Elsevier B.V. on behalf of King Saud University. This is an open access article under the CC BY-NC-ND license (<http://creativecommons.org/licenses/by-nc-nd/4.0/>).

## 1. Introduction

The ongoing COVID-19 global pandemic has caused nations health, economic, and social crises. COVID-19 is uncommon pneumonia caused by SARS-CoV-2 (Ji et al., 2020; Vale et al., 2021), a virus belonging to the family Coronaviridae. SARS-CoV-2 is more contagious than other coronavirus such as SARS-CoV and the Middle East respiratory syndrome coronavirus (MERS-CoV) (Vale et al., 2021; Zhu et al., 2020). As of 20 May 2022, more than 522 million confirmed COVID-19 globally (WHO, 2022). Early data have indicated that approximately 20% of COVID-19 patients require hospitalization, including 5% admitted to the intensive care unit (Koyama et al., 2020). The fatality rate for COVID-19 in the world is 1.2% (data per 20 May 2022) (WHO, 2022), which is lower than SARS (9.6%) and MERS (34.3%) (Koyama et al., 2020). COVID-19 mortality is higher in people with comorbidities such as chronic lung disease, diabetes, heart disease, hypertension, and obesity (Nikolic et al., 2021). Controlling COVID-19 presents a major challenge because the disease often presents symptoms similar to colds and flu, thus hindering diagnosis (Song et al., 2021; Tymms et al., 2020; Woo et al., 2020).

Moreover, COVID-19 causes asymptomatic infections characterized by the positive detection of the SARS-CoV-2 nucleic acid in patient samples and the lack of typical clinical symptoms and apparent abnormalities in lung computed tomography (CT) (Mizumoto et al., 2020). Asymptomatic individuals can transmit the virus to others, which poses a great danger because no specific signs or symptoms are observed (Daniel et al., 2021; McRae et al., 2020). Early November 2021, scientists identified a new variant of the SARS-CoV-2 in Botswana (known as Omicron) and has since turned up in a traveler arriving in Hong Kong from South Africa (Callaway, 2021). Identifying new strains is not easy, and proper methods are essential to prevent the spread of COVID-19 (Afzal, 2020; Ji et al., 2020; Song et al., 2021).

RT-qPCR is the most common method for COVID-19 diagnosis. This method has good accuracy without any interference from other viruses (Babady et al., 2021). However, RT-qPCR is relatively time-consuming (approximately 2 h), and the results are obtained after 1 to 3 days (Ji et al., 2020). This technology also needs an experienced laboratory technician and requires repeated measurements for a valid result (Cui and Zhou, 2020; Song et al., 2021). Another disadvantage of the RT-qPCR method is a high false-negative rate (46.3%) (Pan et al., 2020). Individuals with false-negative results may contribute significantly to the virus spread, thus hampering effective infection control. RT-qPCR can detect SARS-CoV-2 in both symptomatic and asymptomatic patients. However, new cases related to SARS-CoV-2 gene mutations are reported to be undetected using at least one of the commercialized primers (Afzal, 2020). As gene mutations alter viral RNA sequences, new targets need to be detected. Effective assays and reagents pose a challenge for detecting new targets using RT-qPCR. Developing appropriate assays and reagents requires advanced research, which may be time-consuming. Other standard methods, i.e., chest computed tomography (chest CT) and lateral flow immunoassays, are used for symptomatic patients (Cavaleria et al., 2021; Wang et al., 2020). Several days are needed to confirm that a

patient is infected with SARS-CoV-2. Therefore, various methods have been introduced as alternatives to replace the standard techniques. One of these methods is fluorescence spectroscopy.

Fluorescence spectroscopy has good selectivity and sensitivity and is a rapid, cost-effective, simple, and non-destructive method (Diao et al., 2020). It is a perfect candidate for the detection of COVID-19 in clinical samples (Barauna et al., 2020; Khan and Rehman, 2020). The samples fluoresce under a light source in a visible light range and produce a response in the form of fluorescence as excitation and emission peaks (Fardiyah et al., 2020; Juniawan et al., 2020). The physicochemical properties of viruses can serve as unique markers that could be detected via fluorescence emission. Although gene mutations may change the physicochemical properties of viruses (Bakhshandeh et al., 2021), these changes can still be detected by fluorescence spectrophotometry. It can be detected because the presence of the virus in infected individuals remains specific enough to distinguish them from uninfected individuals. Thus, fluorescence analysis of the intact virus could help identify the coronavirus family. Various samples can be tested without requiring a complicated preparation process.

Some researchers have used fluorescence spectrophotometry to diagnose coronaviruses but with other techniques. Diao et al. developed an immunochromatographic fluorescence assay for detecting the nucleocapsid gene (N gene) of SARS-CoV-2 (Diao et al., 2020). This assay could detect COVID-19 in the urine of 73.6% of diagnosed patients based on the presence of the N gene. This technique has a working principle similar to that of a pregnancy test. However, this assay involves some complicated preparation and reagents to enable fluorescence.

Woo et al. reported a sensitive fluorescence detection assay for SARS-CoV-2 RNA in clinical samples using one-pot isothermal ligation and transcription (Woo et al., 2020). They used the principle of isothermal amplification for RNA. From their work on 40 nasopharyngeal SARS-CoV-2 samples, the assay reached positive and negative predictive values of 95% and 100%, respectively. However, this assay still needs to extract SARS-CoV-2 RNA, and its purification is often a prerequisite for diagnostic assays based on isothermal RNA amplification methods. It includes four main components, namely probes, SplintR ligase, T7 RNA polymerase, and a fluorogenic dye. The fluorogenic dye is used to bind the RNA aptamer. Their binding stabilizes the planar structure of the fluorogenic dye and facilitates fluorescence emission as an output. This assay enables sensitive RNA detection without pre-amplification steps such as those required in RT-qPCR.

In the present study, fluorescence spectrophotometry was used to investigate nasopharyngeal and oropharyngeal swab samples from individuals with or without COVID-19. This method is simpler, cheaper, and faster than the standard method (RT-qPCR). The performance of the fluorescence spectrophotometry was examined based on the excitation and emission peak wavelengths of the virus protein to differentiate between individuals with and without COVID-19. The method in this work showed a good result and had the potency to be used in routine analysis.

## 2. Materials and methods

### 2.1. Materials

RADI transport medium (RTM) was obtained from KH Medical (Gyeonggi-do, Republic of Korea). RTM is used to collect and transport clinical specimens containing viruses from the collection site to the testing laboratory. Sterile distilled water was obtained from the Institute of Tropical Disease, Airlangga University. The QIAamp Viral RNA mini kit was obtained from QIAGEN, Cat. No. 52,904 (Hilden, Germany). Sulfuric acid (H<sub>2</sub>SO<sub>4</sub>, 98%) and hydrogen peroxide (H<sub>2</sub>O<sub>2</sub>, 30%) were purchased from Merck, Germany. Piranha solution (98% H<sub>2</sub>SO<sub>4</sub>: 30% H<sub>2</sub>O<sub>2</sub> = 3:1) was used for glass apparatus cleaning. Technical ethanol (96%), used for cleaning and disinfecting purposes, was purchased from SAP Chemical, Indonesia.

### 2.2. Sample collection and preparation

The collecting sample procedure in this work has passed the ethical committee of Airlangga University Hospital with ethical clearance number 162/KEP/2021. Clinical swab samples were collected from hospitals throughout East Java, Indonesia, without particular criteria. All patients were treated as per the standard protocol for swab sampling. Sterile cotton swabs (KH Medical, Republic of Korea) were used to probe the patients' nasopharyngeal and oropharyngeal cavities and were immediately placed into a sterile tube containing RTM. The samples were stored below -20 °C and transported to the Institute of Tropical Disease, Airlangga University. In this work, 40 samples were selected randomly. Each sample was divided into two parts. The first part was tested using a standard method, RT-qPCR (ThermoFisher Scientific, ABI 7500), to validate individuals who were positive or negative for COVID-19. The negative and positive samples were coded as N<sub>n</sub> and P<sub>n</sub>, respectively, where n is the data number (1, 2, 3, etc.) generated from the RT-qPCR test.

The second part for fluorescence measurement was prepared by taking 1 mL of the sample and placing it into a fluorescence cuvette. The sample was then diluted with 2 mL sterile distilled water. Finally, the cuvette was sealed with parafilm for safety and subsequent measurement. All preparation steps were conducted in a Biosafety Level III laboratory with the relevant safety protocols for handling SARS-CoV-2.

### 2.3. Assay protocol for swab sample identification by RT-qPCR testing

#### 2.3.1. Nucleic acid extraction

Viral nucleic acids were extracted from 200 µL of clinical samples using the QIAamp Viral RNA mini kit. Briefly, 5 µL of internal control A was added to each clinical sample as the internal control (IC) from the extraction process. The nucleic acid extraction solution was added to the reaction tube within 10 min. The extracted nucleic acid was transferred to a centrifuge tube and stored at -25 - -15 °C for long-term storage.

#### 2.3.2. Reagent preparation and setting conditions for RT-qPCR analysis

2.3.2.1. *Applied biosystems 7500 RT-qPCR instrument system.* The PCR mixture was prepared according to Table SM1, and 21 µL was dispensed into each PCR tube. If IC A was added during the extraction process, the mixture was prepared without IC A, and 20 µL of the mixture was dispensed into each PCR tube. (0.5 µL of IC A was added to wells assigned as the positive control (PC) and negative control (NC)).

2.3.2.2. *RT-qPCR amplification.* The PC, NC, and nucleic acids extracted from clinical samples (10 µL) were added to the PCR mixture's respective tubes. The mixture was centrifuged at 3000 rpm for 60 s and then placed on the real-time fluorescence quantitative PCR instrument. The cycle conditions were then set on the PCR instrument for nucleic acid amplification (Table SM2).

### 2.4. Fluorescence analysis of swab samples

Fig. 1 shows the scheme of the fluorescence analysis process used in this work. The fluorescence analysis of all samples was performed using a PerkinElmer LS55 Fluorescence Spectrometer (PerkinElmer, USA) equipped with a standard photomultiplier detector and FL WinLab software. The initial step, i.e., pre-scan, was performed to determine the excitation and emission wavelength at the maximum intensity of the sample (Fardiyah et al., 2020; Juniawan et al., 2020). The pre-scan proceeded at excitation wavelengths of 200–800 nm, then continued at emission wavelengths of 200–900 nm. The pre-scan was conducted five times. The wavelength obtained at the maximum intensity was used for further measurement. The scan condition speed was set at 500 nm/min with excitation and emission monochromator slits of 10 nm. All samples were scanned five times. All data were statistically analyzed using one-way ANOVA and least significant difference (LSD) testing. Further data processing was performed through principal component analysis (PCA).

This method's specificity and accuracy were calculated using equations (1) and (2). Specificity defines as the probability that a test result will be negative when the disease is not present. Whereas accuracy is the total coincidence rate.

$$\text{Specificity}(\%) = \frac{TN}{TN + FP} \times 100 \quad (1)$$

$$\text{Accuracy}(\%) = \frac{TN + TP}{\text{Totalsample}} \times 100 \quad (2)$$

where TN is a true negative, TP is a true positive, and FP is a false positive.

### 2.5. The effect of Ct value in fluorescence analysis

Fluorescence spectrophotometry also was performed to analyze the COVID-19-positive samples with various Ct values. This work aims to know the Ct value effect in the fluorescence spectrum. Nine COVID-19-positive samples with high Ct values (22–33 cycles) were obtained using RT-qPCR identification. For fluorescence measurement, each sample was prepared as described in section 2.2. All samples were analyzed



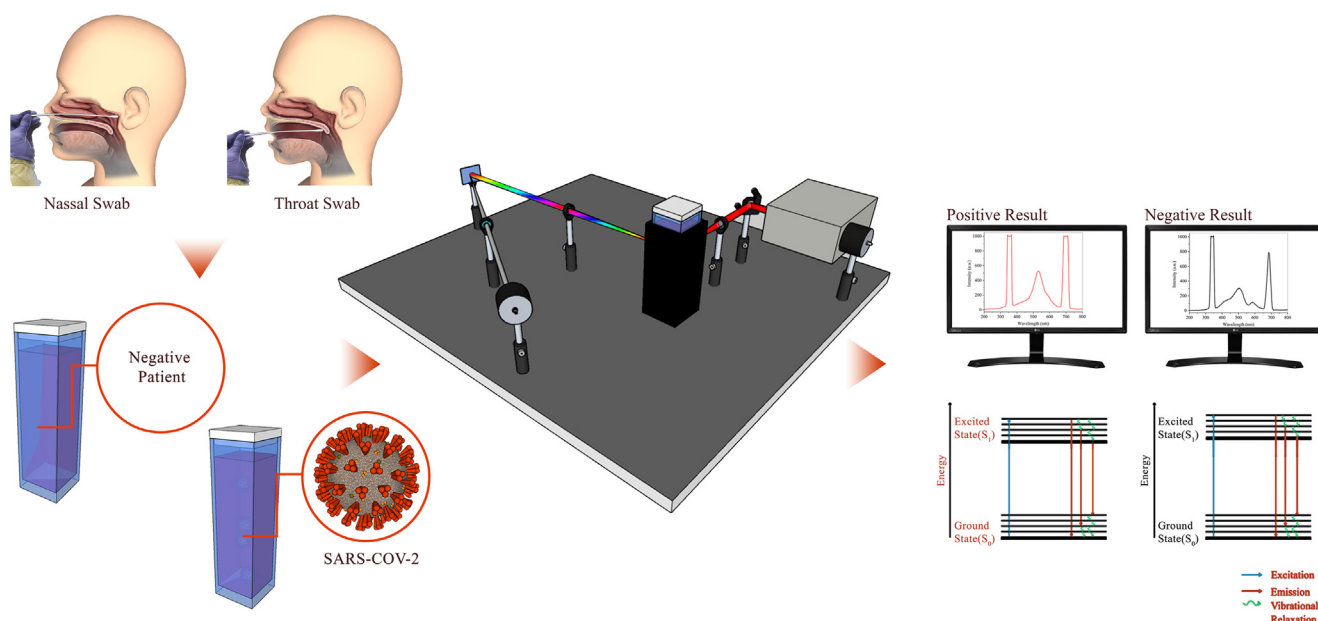


**Fig. 1** Schematic representation of the fluorescence analysis process for detecting COVID-19-negative and -positive samples.

using fluorescence spectrophotometry with steps as explained in section 2.4. All data were analyzed using PCA.

### 3. Results and discussion

#### 3.1. Identification of patients positive and negative for COVID-19

##### 3.1.1. Identification using the standard method (RT-qPCR)

RT-qPCR testing was performed to validate the positive or negative patients for COVID-19. The results of the RT-qPCR assay are shown in Table 1, with the amplification plot shown in Fig. SM1-SM4. In total, 20 samples were negative, and 20 samples were positive for COVID-19.

All positive samples had low Ct (Cycle threshold) values ( $\leq 20$  cycles) for both the envelope protein gene (E gene) and replicase open reading frame 1ab (ORF1ab). The E gene and ORF1ab are biomarkers indicating the presence of SARS-CoV-2 (Al-Qahtani, 2020; Barauna et al., 2020). The results showed that the number of copies of the E gene and ORF1ab was large in the positive samples. A large number of copies indicates a high number of viruses in the sample (Babady et al., 2021). The results from RT-qPCR were then used to validate the fluorescence analysis.

##### 3.1.2. Identification based on fluorescence spectra

In this study, SARS-CoV-2 was detected directly using a fluorescence spectrometer without complicated preparation and chemicals. The 20 positive samples from nasopharyngeal and oropharyngeal swabs could be distinguished from negative samples. This identification was based on the specific emission wavelength. The fluorescence spectra of SARS-CoV-2 are probably a result of the combination of the envelope, the spike (S) protein, E-protein, M-protein, and HE-Protein (Madurani et al., 2021). All these proteins are located on the outer part of the virus and play a critical role in virus detection.

Fluorescence measurement was performed for 20 negative and positive COVID-19 samples based on the RT-qPCR results. The excitation and emission wavelengths at the maximum intensity were obtained from the pre-scan step, and the results are summarized in Table SM3. The average peak excitation wavelength of the negative and positive samples was  $342.71 \pm 0.91$  nm and  $343.17 \pm 8.41$  nm, respectively. Simultaneously, the average peak emission wavelength was  $349.57 \pm 0.98$  nm and  $358.82 \pm 9.06$  nm for the negative and positive samples, respectively. These wavelengths were then used for scanning to determine the profile of fluorescence spectra for negative and positive samples.

The result of the scanning process for fluorescence measurement is shown in Fig. 2. The excitation spectrum (Fig. 2A) is not specific for distinguishing the positive sample from the negative sample. Fig. 2B shows the emission spectra of the negative and positive samples, which showed different small profiles. The sample showed unique fluorescence characteristics, indicated by the emission peak shift in the yellow and blue regions (Fig. 2B). The specific emission wavelength from the sample is listed in Table 2 (the complete data can be seen in Table SM4). Positive samples were observed at an average of  $522.47 \pm 11.78$  nm and  $692.18 \pm 10.89$  nm. Whereas the negative samples were noticed at an average of  $508.37 \pm 5.68$  nm and  $685.27 \pm 0.44$  nm. These emission wavelengths are relatively slight differences, so it is difficult to distinguish positive and negative samples directly from their fluorescence spectra. Therefore, statistical data processing is needed, i.e., the significance test and the multivariate analysis. The significance test was performed using ANOVA and LSD, while the multivariate analysis was analyzed using PCA.

Statistical analysis of both the first and second emission wavelengths using ANOVA showed that the F-calculated value was higher than the F-critical value (Table SM5 and SM6). The null hypothesis is no significant difference between positive and negative wavelengths. Hence, the null hypothesis was rejected, indicating that the measurement data showed

**Table 1** Data of swab samples obtained using RT-qPCR.

No.	Ct value				Conclusion	Sample code for fluorescence analysis
	E gene	Number of copies	ORF1ab	Number of copies		
1.	N/A	N/A	N/A	N/A	Negative	N1
2.	N/A	N/A	N/A	N/A	Negative	N2
3.	N/A	N/A	N/A	N/A	Negative	N3
4.	N/A	N/A	N/A	N/A	Negative	N4
5.	17.34	$1.14 \times 10^6$	15.07	$1.29 \times 10^6$	Positive	P1
6.	15.56	$3.34 \times 10^6$	14.31	$3.04 \times 10^6$	Positive	P2
7.	17.73	$8.96 \times 10^6$	16.77	$0.67 \times 10^6$	Positive	P3
8.	16.24	$2.22 \times 10^6$	15.06	$1.92 \times 10^6$	Positive	P4
9.	17.09	$1.87 \times 10^6$	13.84	$2.32 \times 10^6$	Positive	P5
10.	17.74	$0.55 \times 10^6$	15.58	$0.44 \times 10^6$	Positive	P6
11.	13.90	$4.21 \times 10^6$	12.19	$2.49 \times 10^6$	Positive	P7
12.	19.33	$0.24 \times 10^6$	16.79	$0.24 \times 10^6$	Positive	P8
13.	17.08	$0.78 \times 10^6$	15.05	$0.58 \times 10^6$	Positive	P9
14.	16.93	$0.54 \times 10^6$	15.62	$0.41 \times 10^6$	Positive	P10
15.	16.72	$0.60 \times 10^6$	15.18	$0.51 \times 10^6$	Positive	P11
16.	19.94	$0.11 \times 10^6$	19.06	$0.07 \times 10^6$	Positive	P12
17.	12.61	$5.45 \times 10^6$	11.23	$3.78 \times 10^6$	Positive	P13
18.	18.22	$0.27 \times 10^6$	16.31	$0.29 \times 10^6$	Positive	P14
19.	13.44	$3.48 \times 10^6$	11.89	$2.70 \times 10^6$	Positive	P15
20.	18.76	$0.20 \times 10^6$	17.27	$0.18 \times 10^6$	Positive	P16
21.	18.91	$0.10 \times 10^6$	17.27	$0.08 \times 10^6$	Positive	P17
22.	11.89	$2.10 \times 10^6$	9.88	$1.72 \times 10^6$	Positive	P18
23.	12.59	$1.55 \times 10^6$	10.95	$1.10 \times 10^6$	Positive	P19
24.	8.56	$79.49 \times 10^6$	8.37	$24.00 \times 10^6$	Positive	P20
25.	N/A	N/A	N/A	N/A	Negative	N5
26.	N/A	N/A	N/A	N/A	Negative	N6
27.	N/A	N/A	N/A	N/A	Negative	N7
28.	N/A	N/A	N/A	N/A	Negative	N8
29.	N/A	N/A	N/A	N/A	Negative	N9
30.	N/A	N/A	N/A	N/A	Negative	N10
31.	N/A	N/A	N/A	N/A	Negative	N11
32.	N/A	N/A	N/A	N/A	Negative	N12
33.	N/A	N/A	N/A	N/A	Negative	N13
34.	N/A	N/A	N/A	N/A	Negative	N14
35.	N/A	N/A	N/A	N/A	Negative	N15
36.	N/A	N/A	N/A	N/A	Negative	N16
37.	N/A	N/A	N/A	N/A	Negative	N17
38.	N/A	N/A	N/A	N/A	Negative	N18
38.	N/A	N/A	N/A	N/A	Negative	N19
40.	N/A	N/A	N/A	N/A	Negative	N20

precision with a significant 95% confidence interval difference. The LSD test of both the first and second emission peak wavelengths showed a significant difference in the mean data between sample variations (Table SM7 and SM8).

Further data processing was performed using PCA. PCA is an unsupervised technique that reduces the spectral data space to principal components (PCs), responsible for the most variance in the original dataset (Barauna et al., 2020). In contrast, the loading on the first two PCs was used to derive specific biomarkers indicative of the infected and non-infected categories. In this study, for classification models in PCA, the samples were designated from 20 negative and 20 positive samples for COVID-19 according to the RT-qPCR data. The PCA used the full spectrum of emissions from all samples. PCA calculations show significantly different coordinate regions for positive and negative samples on the graph. The results of PCA (Fig. 3) indicate that samples negative for COVID-19 are clustered in a specific area, as shown by the green ellipse.

Conversely, the samples positive for COVID-19 are outside of the green ellipse. Negative samples have a narrower region than the positive samples. The specificity of this work was achieved 100%.

### 3.2. The effect of Ct value in fluorescence analysis

Variations in the Ct value of the COVID-19-positive sample were observed in its influence in fluorescence testing. In this study, nine positive samples with high Ct values have been identified by RT-qPCR, and the result is shown in Table SM9. For fluorescence analysis, the pre-scan data is shown in Table SM10. The excitation and emission wavelength from the pre-scan step were used in the scanning process to know the profile of fluorescence spectra in variations of Ct values. The result of the scanning process in fluorescence measurement is shown in Fig. SM5. The excitation and emission peaks show a similar pattern with the low Ct value (Fig. 2).

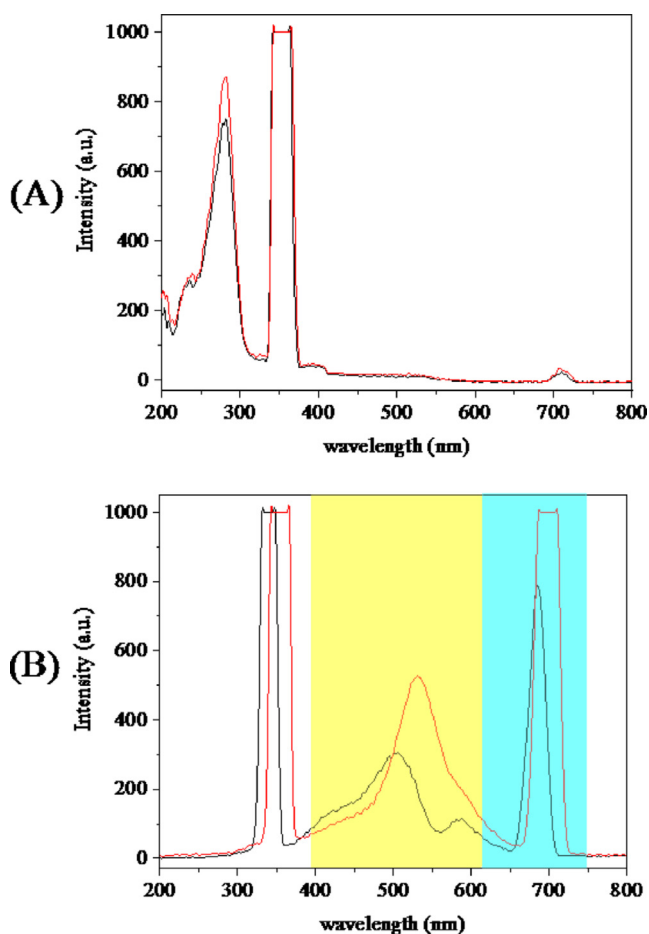


**Fig. 2** Excitation (A) and emission (B) peaks of negative (black) and positive (red) samples. The specific emission wavelength region: the first (yellow area) and the second (blue area).

The multivariate analysis by PCA also proved that the data distributed uniform (Fig. SM6). The lower Ct value means it has a higher viral load. The result means that a small amount of the virus can still be detected. In this work, the LOD obtained 42.20 copies/ml (Ct value of 33.65 cycles) for the E gene and 63.60 copies/ml (Ct value of 31.36 cycles) for ORF1ab.

### 3.3. Performance of fluorescence spectrophotometry for COVID-19 detection

Spectroscopy techniques have attracted much focus for their development as biomedical tools for early diagnosis to monitor human disease (Lukose et al., 2021). The principle underlying this method is based on vibrational spectroscopy, which relies on the molecular vibrations of the chemical structure of

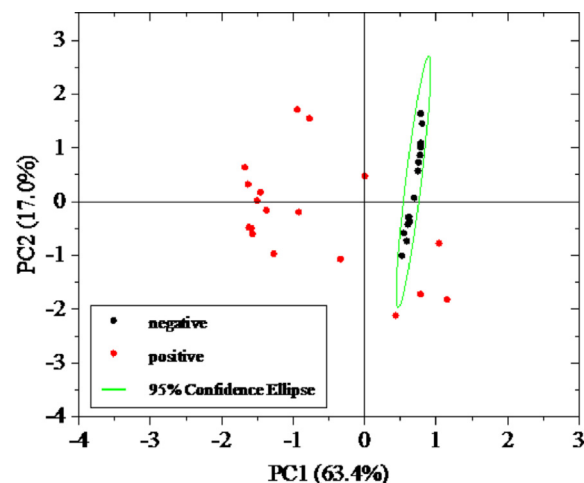


**Fig. 3** Principal component analysis of COVID-19 samples.

molecules (Barauna et al., 2020; Lukose et al., 2021; Madurani et al., 2021; Sivakumar et al., 2021). Infrared (Barauna et al., 2020; Mayerhöfer et al., 2021) and Raman (Desai S et al., 2020; Hernández-Arteaga et al., 2022) spectroscopies are reported to be capable of assisting in the diagnosis of infection caused by SARS-CoV-2. From intact viruses, biomolecules, such as DNA, RNA, proteins, and lipids, can produce unique spectral vibrations based on their structural heterogeneity.

Moreover, conventional fluorescence spectrophotometry has not been explored widely but seems promising for future technologies. According to our results, we propose that this technique can be applied to detecting other pathogens. First, it is a simple technique that requires no complicated preparation steps. Second, it is a rapid analysis that only takes 4 min to detect the infection (Table 3). Third, the accuracy (total coincidence rate) was calculated with equation (2), which reached 100% for this work. RT-qPCR has high accuracy (84–98%) compared to standard methods, but this method needs approximately two hours to obtain the result. The accuracy of other standard methods such as chest CT and lateral flow immunoassay is shown to be approximately 68% and 97%, respectively. The performance of alternative spectroscopy methods such as ATR-infrared, Raman spectroscopy, fluorescence immunochromatography, and sensitive fluorescence-based on one-pot isothermal RNA detection is not more accurate than that of the proposed method (Table 3).

This work shows an excellent result for 40 samples. All the positive samples can be distinguished from the negative samples. Expanding to more samples can help to check how accurate this method is. It allows further development and validation of the fluorescence spectrophotometry technique. The limitation of this study is only used to identify samples from COVID-19 patients, ignoring the possible congenital dis-

**Table 2** Specific emission peak wavelengths of samples negative and positive for COVID-19.

Sample group	Wavelengths (nm)	
	Average of the first emission peak	Average of the second emission peak
Negative	508.37 ± 5.68	685.27 ± 0.44
Positive	522.47 ± 11.78	692.18 ± 10.89

**Table 3** Performance of several methods for COVID-19 detection.

Method	Accuracy	Analysis time	Specificity	Limit of detection	Ref.
RT-qPCR	84–98%	~2 h	97–100%	1.20 copies/ml	Fukasawa et al., 2021
Chest CT	68%	several days	N/A	N/A	Fang et al., 2020
Lateral flow immunoassay	95–97%	2–5 min	95–100%	N/A	Cavalera et al., 2021
ATR-Infrared	90%	2–5 min	89%	1582 copies/ml	Barauna et al., 2020
Raman spectroscopy	91.6%	2–5 min	88.8%	N/A	Desai S et al., 2020
Fluorescence immunochromatography	73%	4 min	100%	N/A	Diao et al., 2020
Sensitive fluorescence-based on one-pot isothermal RNA detection	95%	30–50 min	N/A	aM	Woo et al., 2020
Fluorescence spectrophotometry	100%	4 min	100%	42.20 copies/ml for E gene and 63.60 copies/ml for ORF1ab	This work

eases. This method can be developed to test in various interferences samples. In addition to its sensitivity, application to other pathogens and specificity to each pathogen can be evaluated. Fluorescence spectrophotometry can be combined with several techniques to improve the accuracy of diagnosis. This technique can also be developed for system miniaturization. Furthermore, it can be connected to smart devices, such as smartphones, for portable testing. Portable technologies would facilitate its use in hospitals, clinics, airports, stations, and other high-traffic areas as well as at home.

#### 4. Conclusions

Overall, our results demonstrate that fluorescence spectrophotometry is advantageous for SARS-CoV-2 detection compared to other detection methods. Clinical swab samples from the positive or negative patients can be identified directly based on their fluorescence spectral profile depending on the physicochemical characteristics of the viral protein in RTM. They have significantly different emission wavelengths. All positive samples could be clearly distinguished from negative samples using fluorescence spectrophotometry. This measurement only took 4 min. The detection limit of this work is 42.20 copies/ml for the E gene and 63.60 copies/ml for ORF1ab with 100% in specificity and accuracy. We thus propose that fluorescence spectrophotometry be promoted as a potential technique for COVID-19 detection. An increase in the number of samples is required for future research.

#### 5. Data statement

The research data is confidential.

#### CRediT authorship contribution statement

**Kartika A. Madurani:** Conceptualization, Methodology, Data curation, Writing – original draft. **Suprpto Suprpto:** Conceptualization, Methodology, Data curation, Writing – original draft. **Muhammad Yudha Syahputra:** Conceptualization, Methodology, Data curation, Writing – original draft. **Ika Puspita:** Visualization, Investigation. **Abdul Hadi Furqoni:** Visualization, Investigation. **Listya Puspasari:** Visualization, Investigation. **Hafildatur Rosyidah:** Visualization, Investigation. **Agus Muhamad Hatta:** Software, Validation. **Juniastuti Juniastuti:** Software, Validation. **Maria Inge Lusida:** Software, Validation. **Masato Tominaga:** Writing – original draft. **Fredy Kurniawan:** Supervision.

#### Declaration of Competing Interest

The authors declare that they have no known competing financial interests or personal relationships that could have appeared to influence the work reported in this paper.

#### Acknowledgments

The authors acknowledge the ethical committee of Universitas Airlangga Hospital for ethical clearance in this research. Grateful to Dra. Ita Ulfin, M.Si. as the Head of Laboratory of Instrumentation and Analytical Science, Chemistry Department, Faculty of Science and Data Analytics, Institut Teknologi Sepuluh Nopember and ITD Airlangga University for laboratory facilities. Acknowledgments are also given to Mochammad Zakki Fahmi, Ph.D., and Dr. Hendro Juwono, M.Si, for fruitful discussion.

#### Funding

The Indonesian Government supported this work, especially the National Agency for Research and Innovation (BRIN) and the Ministry of Finance under Lembaga Pengelola Dana Pendidikan (LPDP), under the project scheme of Research and Innovation Consortium for COVID-19 [BRIN decree ID 60/II/HK/2022] and dissertation scheme [grant number PRJ-46/LPDP.4/2020].

#### Appendix A. Supplementary material

Supplementary data to this article can be found online at <https://doi.org/10.1016/j.arabjc.2022.104020>.

#### References

- Afzal, A., 2020. Molecular diagnostic technologies for COVID-19: Limitations and challenges. *J. Adv. Res.* 26, 149–159. <https://doi.org/10.1016/j.jare.2020.08.002>.
- Al-Qahtani, A.A., 2020. Severe acute respiratory syndrome coronavirus 2 (SARS-CoV-2): emergence, history, basic and clinical aspects. *Saudi J. Biol. Sci.* 27, 2531–2538. <https://doi.org/10.1016/j.sjbs.2020.04.033>.
- Babady, N.E., McMillen, T., Jani, K., Viale, A., Robilotti, E.V., Aslam, A., Diver, M., Sokoli, D., Mason, G., Shah, M.K.,



- Korenstein, Kamboj, M., 2021. Performance of severe acute respiratory syndrome coronavirus 2 real-time RT-PCR tests on oral rinses and saliva samples. *J. Mol. Diagn.* 23, 3–9. <https://doi.org/10.1016/j.jmoldx.2020.10.018>.
- Bakhshandeh, B., Jahanafrooz, Z., Abbasi, A., Goli, M.B., Sadeghi, M., Mottaqi, M.S., Zamani, M., 2021. Mutations in SARS-CoV-2; consequences in structure, function, and pathogenicity of the virus. *Microb. Pathog.* 154., <https://doi.org/10.1016/j.micpath.2021.104831> 104831.
- Barauna, V.G., Singh, M.N., Barbosa, L.L., Marcarini, W.D., Vassallo, P.F., Mill, J.G., Ribeiro-Rodrigues, R., Warnke, P.H., Martin, F.L., 2020. Ultra-rapid on-site detection of SARS-CoV-2 infection using simple ATR-FTIR spectroscopy and analysis algorithm: high sensitivity and specificity. *Anal Chem* 93, 2950–2958. <https://doi.org/10.1101/2020.11.02.20223560>.
- Callaway, E., 2021. Heavily mutated coronavirus variant puts scientists on alert. *Nature*. <https://doi.org/10.1038/d41586-021-03552-w>.
- Cavalera, S., Colitti, B., Rosati, S., Ferrara, G., Bertolotti, L., Nogarol, C., Guiotto, C., Cagnazzo, C., Denina, M., Fagioli, F., Di Nardo, F., Chiarello, M., Baggiani, C., Anfossi, L., 2021. A multi-target lateral flow immunoassay enabling the specific and sensitive detection of total antibodies to SARS COV-2. *Talanta* 223., <https://doi.org/10.1016/j.talanta.2020.121737> 121737.
- Cui, F., Zhou, H.S., 2020. Diagnostic methods and potential portable biosensors for coronavirus disease 2019. *Biosens. Bioelectron.* 165., <https://doi.org/10.1016/j.bios.2020.112349> 112349.
- Daniel, E.A., Esakialraj L, B.H., S, A., Muthuramalingam, K., Karunaianantham, R., Karunakaran, L.P., Nesakumar, M., Selvachithiram, M., Pattabiraman, S., Natarajan, S., Tripathy, S.P., Hanna, L.E., 2021. Pooled Testing Strategies for SARS-CoV-2 diagnosis: A comprehensive review. *Diagn. Microbiol. Infect. Dis.* 101, 115432. <https://doi.org/10.1016/j.diagmicrobio.2021.115432>.
- Desai S, Mishra Sv, Joshi A, Sarkar D, Hole A, Mishra R, Dutt S, Chilakapati Mk, Gupta S, Dutt A, 2020. Raman spectroscopy-based detection of RNA viruses in saliva: A preliminary report. *J. Biophotonics* 13, e202000189–e202000189. <https://doi.org/10.1002/jbio.202000189>.
- Diao, B., Wen, K., Chen, J., Liu, Y., Yuan, Z., Han, C., Chen, J., Pan, Y., Chen, L., Dan, Y., Wang, J., Chen, Y., Deng, G., Zhou, H., Wu, Y., 2020. Diagnosis of acute respiratory syndrome coronavirus 2 infection by detection of nucleocapsid protein (preprint). *Epidemiology*. <https://doi.org/10.1101/2020.03.07.20032524>.
- Fang, Y., Zhang, H., Xie, J., Lin, M., Ying, L., Pang, P., Ji, W., 2020. Sensitivity of chest CT for COVID-19: comparison to RT-PCR. *Radiology* 296, E115–E117. <https://doi.org/10.1148/radiol.202000432>.
- Fardiyah, Q., Ersam, T., Suyanta, Slamet, A., Suprpto, Kurniawan, F., 2020. New potential and characterization of *Andrographis paniculata* L. Ness plant extracts as photoprotective agent. *Arab. J. Chem.* 13, 8888–8897. <https://doi.org/10.1016/j.arabjc.2020.10.015>.
- Fukasawa, L.O., Sacchi, C.T., Gonçalves, M.G., Lemos, A.P.S., Almeida, S.C.G., Caterino-de-Araujo, A., 2021. Comparative performances of seven quantitative reverse-transcription polymerase chain reaction assays (RT-qPCR) for detecting SARS-CoV-2 infection in samples from individuals suspected of COVID-19 in São Paulo. Brazil. *J. Clin. Virol. Plus* 1., <https://doi.org/10.1016/j.jcvp.2021.100012> 100012.
- Hernández-Artega, A.C., Ojeda-Galván, H.J., Rodríguez-Aranda, M.C., Toro-Vázquez, J.F., Sánchez, J., José-Yacamán, M., Navarro-Contreras, H.R., 2022. Determination of the denaturation temperature of the Spike protein S1 of SARS-CoV-2 (2019 nCoV) by Raman spectroscopy. *Spectrochim. Acta. A. Mol. Biomol. Spectrosc.* 264., <https://doi.org/10.1016/j.saa.2021.120269> 120269.
- Ji, T., Liu, Z., Wang, G., Guo, X., Akbar Khan, S., Lai, C., Chen, H., Huang, S., Xia, S., Chen, B., Jia, H., Chen, Y., Zhou, Q., 2020. Detection of COVID-19: A review of the current literature and future perspectives. *Biosens. Bioelectron.* 166, 112455. <https://doi.org/10.1016/j.bios.2020.112455>.
- Juniawan, A., Suprpto, Efendi, M.H., Retnowati, R., Kurniawan, F., 2020. Study on fluorescence spectra: characteristics of broiler and pig blood. *IOP Conf. Ser. Earth Environ. Sci.* 493, 012029. <https://doi.org/10.1088/1755-1315/493/1/012029>.
- Khan, R.S., Rehman, I.U., 2020. Spectroscopy as a tool for detection and monitoring of Coronavirus (COVID-19). *Expert Rev. Mol. Diagn.* 20, 647–649. <https://doi.org/10.1080/14737159.2020.1766968>.
- Koyama, T., Platt, D., Parida, L., 2020. Variant analysis of SARS-CoV-2 genomes. *Bull. World Health Organ.* 98, 495–504. <https://doi.org/10.2471/BLT.20.253591>.
- Lukose, J., Chidangil, S., George, S.D., 2021. Optical technologies for the detection of viruses like COVID-19: Progress and prospects. *Biosens. Bioelectron.* 178., <https://doi.org/10.1016/j.bios.2021.113004> 113004.
- Madurani, K.A., Suprpto, S., Syahputra, M.Y., Puspita, I., Masudi, A., Rizqi, H.D., Hatta, A.M., Juniastuti, J., Lusida, M.I., Kurniawan, F., 2021. Review—recent development of detection methods for controlling COVID-19 outbreak. *J. Electrochem. Soc.* 168., <https://doi.org/10.1149/1945-7111/abe9cc> 037511.
- Mayerhöfer, T.G., Pahlow, S., Popp, J., 2021. Recent technological and scientific developments concerning the use of infrared spectroscopy for point-of-care applications. *Spectrochim. Acta. A. Mol. Biomol. Spectrosc.* 251., <https://doi.org/10.1016/j.saa.2020.119411> 119411.
- McRae, M.P., Simmons, G.W., Christodoulides, N.J., Lu, Z., Kang, S. K., Fenyó, D., Alcorn, T., Dapkins, I.P., Sharif, I., Vurmaz, D., Modak, S.S., Srinivasan, K., Warhadpande, S., Shrivastav, R., McDevitt, J.T., 2020. Clinical decision support tool and rapid point-of-care platform for determining disease severity in patients with COVID-19. *Lab. Chip* 20, 2075–2085. <https://doi.org/10.1039/D0LC00373E>.
- Mizumoto, K., Kagaya, K., Zarebski, A., Chowell, G., 2020. Estimating the asymptomatic proportion of coronavirus disease 2019 (COVID-19) cases on board the Diamond Princess cruise ship, Yokohama, Japan, 2020. *Eurosurveillance* 25, 2000180. <https://doi.org/10.2807/1560-7917.ES.2020.25.10.2000180>.
- Nikolic, M., Simovic, S., Novkovic, L., Jokovic, V., Djokovic, D., Muric, N., Bazic Sretenovic, D., Jovanovic, J., Pantic, K., Cekerevac, I., 2021. Obesity and sleep apnea as a significant comorbidities in COVID-19 — A case report. *Obes. Res. Clin. Pract.* <https://doi.org/10.1016/j.orcp.2021.04.008>.
- Pan, Y., Long, L., Zhang, D., Yuan, T., Cui, S., Yang, P., Wang, Q., Ren, S., 2020. Potential False-Negative Nucleic Acid Testing Results for Severe Acute Respiratory Syndrome Coronavirus 2 from Thermal Inactivation of Samples with Low Viral Loads. *Clin. Chem.* 66, 794–801. <https://doi.org/10.1093/clinchem/hvaa091>.
- Sivakumar, R., Dinh, V.P., Lee, N.Y., 2021. Ultraviolet-induced in situ gold nanoparticles for point-of-care testing of infectious diseases in loop-mediated isothermal amplification. *Lab. Chip* 21, 700–709. <https://doi.org/10.1039/D1LC00019E>.
- Song, Q., Sun, X., Dai, Z., Gao, Y., Gong, X., Zhou, B., Wu, J., Wen, W., 2021. Point-of-care testing detection methods for COVID-19. *Lab. Chip* 21, 1634–1660. <https://doi.org/10.1039/D0LC01156H>.
- Tymm, C., Zhou, J., Tadimety, A., Burklund, A., Zhang, J.X.J., 2020. Scalable COVID-19 detection enabled by lab-on-chip biosensors. *Cell. Mol. Bieng.* 13, 313–329. <https://doi.org/10.1007/s12195-020-00642-z>.
- Vale, F.F., Vitor, J.M.B., Marques, A.T., Azevedo-Pereira, J.M., Anes, E., Goncalves, J., 2021. Origin, phylogeny, variability and epitope conservation of SARS-CoV-2 worldwide. *Virus Res.* 304., <https://doi.org/10.1016/j.virusres.2021.198526> 198526.
- Wang, Z., Zheng, Z., Hu, H., Zhou, Q., Liu, W., Li, X., Liu, Z., Wang, Y., Ma, Y., 2020. A point-of-care selenium nanoparticle-based test for the combined detection of anti-SARS-CoV-2 IgM and IgG in

- human serum and blood. *Lab. Chip* 20, 4255–4261. <https://doi.org/10.1039/D0LC00828A>.
- WHO, 2022. WHO Coronavirus (COVID-19) Dashboard. URL <https://covid19.who.int> (accessed 5.23.22).
- Woo, C.H., Jang, S., Shin, G., Jung, G.Y., Lee, J.W., 2020. Sensitive fluorescence detection of SARS-CoV-2 RNA in clinical samples via one-pot isothermal ligation and transcription. *Nat. Biomed. Eng.* 4, 1168–1179. <https://doi.org/10.1038/s41551-020-00617-5>.
- Zhu, X., Ge, Y., Wu, T., Zhao, K., Chen, Y., Wu, B., Zhu, F., Zhu, B., Cui, L., 2020. Co-infection with respiratory pathogens among COVID-2019 cases. *Virus Res.* 285,. <https://doi.org/10.1016/j.virusres.2020.198005> 198005.